One-Pot Template Synthesis and Properties of a Molecular Bowl: Dodecaaza Macrotetracycle with μ_3-Oxo and μ_3-Hydroxo Tricopper(II) Cores

Myunghyun Paik Suh,* Mi Young Han, Jea Ho Lee, Kil Sik Min, and Changbong Hyeon

Department of Chemistry Education
Seoul National University, Seoul 151-742, Korea

Received July 1, 1997

One-pot metal template condensation reactions of formaldehyde and amines provide simple, selective, and inexpensive routes toward the macrocyclic complexes that are not obtainable in the absence of metal ion.[1,2] However, most of the compounds thus prepared are rather small macrocycles containing one or two metal ions. Compounds incorporating big macrocycles or multi metal ions or both have not been prepared thus far from this reaction. In addition, the chemistry of polynuclear Cu(II) complexes is interesting due to the presence of multicopper active sites in several oxidases[3] and with respect to the development of new inorganic materials showing molecular ferromagnetism.[4] In this paper, we show that a bowl-shaped dodecaaza macrotetracycle incorporating a Cu_3O core, $[Cu_3(\mathbf{L})(\mu_3\text{-}O)](ClO_4)_4\cdot 2H_2O$, is synthesized from very simple one-pot template condensation as described in eq 1.[5,6] The $[Cu_3(\mathbf{L})(\mu_3\text{-}O)]^{4+}$ is protonated in an aqueous solution to give $[Cu_3(\mathbf{L})(\mu_3\text{-}OH)]^{5+}$ whose pK_a value is estimated to be 4.6. X-ray structures of $[Cu_3(\mathbf{L})(\mu_3\text{-}O)](ClO_4)_4\cdot 2H_2O$ (**1**) and $[Cu_3(\mathbf{L})(\mu_3\text{-}OH)]Cl_{0.5}(ClO_4)_{4.5}\cdot 1.5H_2O$ (**2**) were determined. The former is one of the rare structurally characterized examples of an oxo-bridged Cu(II) species.[7] Both **1** and **2** show unusual magnetic behavior of mixed ferro- and antiferromagnetic interactions.

$$Cu^{2+} + N(CH_2CH_2NH_2)_3 + CH_2O \rightarrow [Cu_3(\mathbf{L})(\mu_3\text{-}O)]^{4+} \quad (1)$$

The complex **1** was prepared as described.[8] ORTEP views of the cation in **1** are presented in Figure 1.[9,10] There are two independent cations in the structure because of the position of a lattice water molecule, which are related by the noncrystallographic 6-fold screw symmetry. The molecular bowl **L** accommodates three Cu(II) ions which are bonded to a central oxo ion and located at the corners of an equilateral triangle of side 3.125(2) Å for Cu(1) and 3.105(2) Å for Cu(2). The central μ_3-

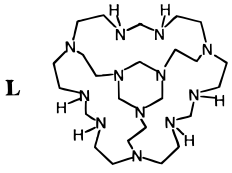

oxygen is on a C_3 axis of the molecule. It is 0.539(8) and 0.528(9) Å above the trigonal planes made by three Cu(1) and three Cu(2) atoms, respectively. The geometry of each copper(II) ion is best described as a distorted trigonal bipyramid (tbp). The basal plane consists of two secondary and one tertiary nitrogen originating from primary amines of tren while the apical sites are occupied by μ_3-oxygen and the central nitrogen of a tren unit. The copper atom is displaced from the trigonal plane toward the apical μ_3-oxygen by 0.238(5) Å for Cu(1) and 0.230(4) Å for Cu(2). The μ_3-oxygen displays sp^3 hybridization with Cu−O−Cu angle of 112°. In the trigonal plane, the N_{sec}−Cu−N_{sec} angle is 121° (av) but two N_{ter}−Cu−N_{sec} angles, 132° (av) and 104° (av), are significantly deviated from the ideal geometry. The axial bonds [av Cu−O_{ax} = 1.876(2) Å, av Cu−N_{ax} = 2.042(5) Å] are shorter than the equatorial [av Cu−N_{eq} = 2.177(3) Å], which may be attributed to the tbp ligand field splitting of Cu(II) having an electron in the d_{z^2} orbital.

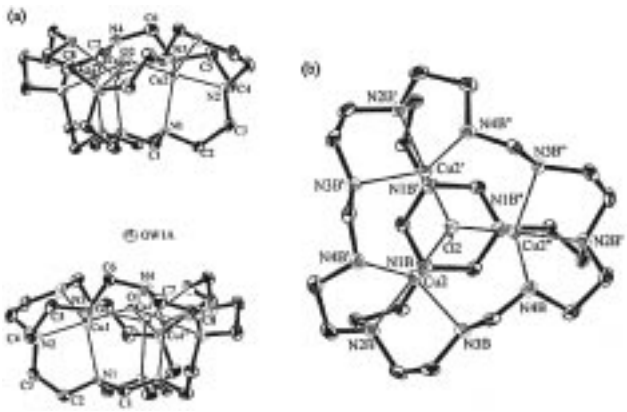

Figure 1. ORTEP drawings of **1**: (a) side view, (b) top view. The 3-fold rotation related atoms are designated by a prime for *z*,*x*,*y* and a double prime for *y*,*z*,*x*. The atoms are represented by 30% probable thermal ellipsoid.[10]

The electronic absorption spectrum of **1** is pH dependent as shown in Figure 2. The complex shows a maximum absorption at 634 nm. At pH < 6, the peak at 634 nm decreases, and a new one appears at 738 nm whose intensity is increased as pH is lowered. The pH-dependent absorption changes of **1** were measured at 738 nm, and pK_a value of 4.65 was estimated from the best fitting curve for the protonated species $[Cu_3(\mathbf{L})(\mu_3\text{-}OH)]^{5+}$.[11] The complex **1** strongly resists decomposition even

(1) (a) For review, see: Suh, M. P. *Advanced Inorganic Chemistry*; Sykes, A. G., Ed.; Academic Press: New York, 1997; Vol. 44, pp 93−146. (b) Suh, M. P.; Kim, S. K. *Inorg. Chem.* **1993**, *32*, 3562. (c) Suh, M. P.; Kim, I. S.; Shim, B. Y.; Hong, D.; Yoon, T.-S. *Inorg. Chem.* **1996**, *35*, 3595. (d) Geue, R. J.; Hambley, T. W.; Harrowfield, J. M.; Sargeson, A. M.; Snow, M. R. *J. Am. Chem. Soc.* **1984**, *106*, 5478. (e) Bertoncello, K.; Fallon, G. D.; Hodgkin, J. H.; Murray, K. S. *Inorg. Chem.* **1988**, *27*, 4750.

(2) (a) Suh, M. P.; Kang, S. *Inorg. Chem.* **1988**, *27*, 2544. (b) Suh, M. P.; Shim, B. Y.; Yoon, T.-S. *Inorg. Chem.* **1994,** *33*, 5509.

(3) *Encyclopedia of Inorganic Chemistry;* King, R. B., Ed.; John Wiley and Sons: New York, 1994; Vol. 2, pp 822−924.

(4) *Molecular Magnetism;* Kahn, O., Ed.; VCH: New York, 1993.

(5) The same condensation with Ni(II) and Co(II) provides completely different macrocycles.[6]

(6) (a) Kang, S. G.; Ryu, K.; Suh, M. P.; Jeong, J. W. *Inorg. Chem.* **1997**, 36, 2478. (b) Suh, M. P.; Lee, J. H.; Han, M. Y.; Yoon, T. S. *Inorg. Chem.* **1997**, 5651.

(7) Butcher, R. J.; O'Connor, C. J.; Sinn, E. *Inorg. Chem.* **1981**, *20*, 537.

(8) To the MeOH solution (100 mL) of $CuCl_2\cdot 2H_2O$ (1.81 g, 10.3 mmol) were added tris(2-aminoethyl)amine (3.14 g, 20.6 mmol) and paraformaldehyde (3.0 g, 100 mmol). The dark blue mixture was heated at reflux for 70 h during which time the solution gradually became green. The solution was allowed to stand at room temperature until green precipitate of $[Cu_3(\mathbf{L})(\mu_3\text{-}O)]Cl_4\cdot 2H_2O$ (**1a**) formed, which was filtered off, washed with EtOH (20 mL), and dried *in vacuo*. {Yield: 51%. Anal. Calcd for $Cu_3C_{24}H_{58}N_{12}Cl_4O_3$ (**1a**): C, 32.20; H, 6.53; N, 18.77. Found: C, 32.09; H, 6.58; N, 18.12.} The Cl^- anion was changed to ClO_4^- by dissolving **1a** (1.30 g) in MeOH/H_2O (9:1 v/v, 30 mL) and then adding a saturated aqueous solution of excess $LiClO_4$ (3.0 g). The solution was heated, hot filtered, and then allowed to stand at room temperature for 1 day. Dark green crystals of **1** formed were filtered, washed with EtOH, and dried *in vacuo*. Anal. Calcd for **1**, $Cu_3C_{24}H_{58}N_{12}Cl_4O_{19}$: C, 25.04; H, 5.08; N, 14.60. Found: C, 25.20; H, 5.20; N, 14.74. ν(NH): 3230 cm^{-1}. Λ_M (H_2O): 491 Ω^{-1} cm^2 M^{-1} for 5.15 × 10^{-4} M. UV/vis (λ_{max}, ϵ): 851 nm (ϵ = 571) and 623 nm (ϵ = 791) in MeCN; 848 nm (ϵ = 545) and 635 nm (ϵ = 665) in H_2O.

(9) Johnson, C. K. ORTEPII. Report ORNL-5138; Oak Ridge National Laboratory, Oak Ridge, TN, 1976.

(10) Crystal data for **1**: $Cu_3C_{24}H_{58}N_{12}Cl_4O_{19}$, fw = 1151.24, cubic, space group $P2_13$, a = 20.443(3) Å, V = 8543.5(22) Å^3, Z = 8, d_{calcd} = 1.790 g cm^{-3}, μ(Mo Kα) = 1.818 mm^{-1}, R = 0.0432 (4σ data), and $wR(F^2)$ = 0.0927. Relevant bond distances (Å) and angles (deg): Cu(1)−O(1), 1.883(3); Cu(1)−N(1), 2.272(7); Cu(1)−N(2), 2.045(7); Cu(1)−N(3), 2.166(8); Cu(1)−N(4), 2.100(8); Cu(2)−O(2), 1.869(3); Cu(2)−N(1), 2.240(7); Cu(2)−N(2), 2.039(7); Cu(2)−N(3), 2.138(7); Cu(2)−N(4), 2.125(7); Cu(1)−O(1)−Cu(1), 112.2(2); O(1)−Cu(1)−N(2), 179.1(2); N(4)−Cu(1)−N(3), 122.0(3); N(4)−Cu(1)−N(1), 130.9(3); N(3)−Cu(1)−N(1), 103.5(3); Cu(2)−O(2)−Cu(2), 112.3(2); O(2)−Cu(2)−N(2), 177.8(3); N(4)−Cu(2)−N(3), 118.7(3); N(4)−Cu(2)−N(1), 133.5(3); N(3)−Cu(2)−N(1), 104.3(3); Cu(1)···Cu(2), 10.163(2); Cu(1)···Cu(2′), 9.670(2); Cu(1)···Cu(2″), 9.677(2).

S0002-7863(97)02178-1 CCC: $15.00
Published on Web 04/04/1998

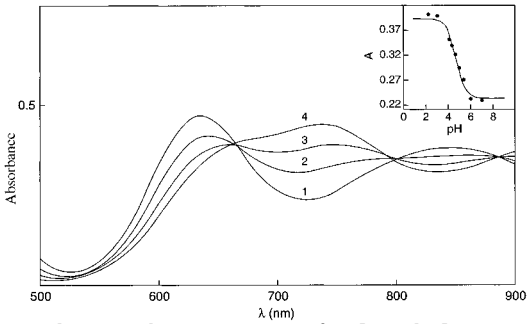

Figure 2. Electronic absorption spectra of **1**: [complex] = 5.29×10^{-4} M, (1) pH = 10.8, (2) pH = 4.89, (3) pH = 3.42, and (4) pH = 1.62. Inset: pH-dependent absorption changes at 738 nm, [complex] = 4.99×10^{-4} M. Solid line is the best fit curve.

Table 1. Structural Comparison between **1** and **2**

	1, $Cu_3(\mu_3-O)$, Å		**2**, $Cu_3(\mu_3-OH)$, Å	
distance	$Cu_3(1)$	$Cu_3(2)$	$Cu_3(1)$	$Cu_3(2)$
Cu−O	1.883(3)	1.869(3)	1.951(4)	1.966(4)
Cu−N_{ax}	2.045(7)	2.039(7)	2.013(9)	2.001(9)
av Cu−N_{eq}	2.188(4)	2.168(4)	2.145(5)	2.140(5)
O from Cu_3 plane	0.539(8)	0.528(9)	0.537(12)	0.564(12)
Cu from N_3 plane	0.238(5)	0.230(4)	0.166(6)	0.164(5)

in 0.4 M $HClO_4$ as verified spectrophotometrically, and we could not obtain the salt of metal-free **L** by the addition of acid to an aqueous or MeCN solution of **1**.

The complex **2** was prepared[12] as blue-green crystals by addition of $HClO_4$ to the aqueous solution of $[Cu_3(\mathbf{L})(\mu_3\text{-O})]Cl_4\cdot 2H_2O$ to a pH of 2, and its crystal structure was determined.[13] The overall structure of **2** is essentially same as that of **1** except that a chloride anion instead of a water molecule locates between the two Cu_3 cluster units. The hydrogen atoms of μ_3-OH in $Cu_3(1)$ and $Cu_3(2)$ cluster units are hydrogen bonded with a Cl^- anion and an oxygen atom of ClO_4^-, respectively, which is reflected in the low ν(OH) values. Structural data of μ_3-oxo and μ_3-hydroxo complexes are compared in Table 1. Upon protonation, the Cu−O bonds are significantly lengthened (ca. 0.07−0.1 Å), while the Cu−N_{ax} bonds are shortened (ca 0.03 Å). In the $[Cu_3(\mathbf{L})(\mu_3\text{-OH})]^{5+}$ cation, the $Cu_3(1)$ cluster unit shows longer Cu−O and shorter Cu−N_{ax} bond distances than the $Cu_3(2)$ unit, indicating that the hydrogen bond between the μ_3-OH of $Cu_3(1)$ cluster and a Cl^- anion is stronger than that between the μ_3-OH of $Cu_3(2)$ cluster and an oxygen atom of ClO_4^-.

Magnetic susceptibilities of **1** and **2** were measured in the range of 2−300 K with a SQUID magnetometer and are plotted in Figure 3.[14] For both complexes, the value of $\chi_M T$ increases with decreasing temperature until it reaches a maximum, indicating a dominant ferromagnetic coupling within the Cu_3 species.[15] At lower temperature, χ_MT decreases rapidly showing the antiferromagnetic coupling, which is associated with the interaction between the trimetallic cluster units.[16] The magnetic data are interpreted in terms of spin Hamiltonian for a Cu_3 unit as described in eq 2. Introducing an intercluster interaction,[16] χ_M per trinuclear cluster is expressed as eq 3 where $F(T) = (e^{-3/2J/kT} + 5)/(e^{-3/2J/kT} + 1)$.[7,17,18]

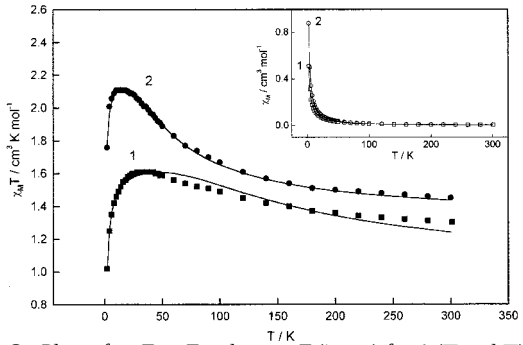

Figure 3. Plots of $\chi_M T$ vs T and χ_M vs T (insert) for **1** (■ and □) and **2** (● and ○) under 1.0 T. The solid lines are the best fit curves to eq 3.

$$\boldsymbol{H} = -J(S_1\cdot S_2 + S_2\cdot S_3 + S_3\cdot S_1) - g\mu_B(S_1 + S_2 + S_3)\cdot H \quad (2)$$

$$\chi_M = Ng^2\mu_B{}^2F(T)/[4kT - zJ'F(T)] \quad (3)$$

The best fit parameters for the magnetic susceptibility data to eq 3 are $g = 1.88$, $J = 109$ cm^{-1}, and $zJ' = -0.720$ cm^{-1} ($R = 3.00 \times 10^{-4}$) for **1**, and $g = 2.17$, $J = 37.8$ cm^{-1}, and $zJ' = -0.260$ cm^{-1} ($R = 5.30 \times 10^{-5}$) for **2**. Although most of the tricopper complexes previously reported exhibited antiferromagnetic interactions[19−21] and few showed ferromagnetism,[22] the present μ_3-oxo and μ_3-hydroxo tricopper complexes show a mixed magnetic behavior with strong intramolecular ferromagnetic interactions and weak intermolecular antiferromagnetic couplings.[16,21,22] The magnetic interactions are much stronger in the μ_3-oxo complex than in the μ_3-hydroxo complex.

Acknowledgment. This work was supported by Korea Science and Engineering Foundation through the Center for Molecular Catalysis and the Basic Research Institute Program (BSRI97-3415), Ministry of Education, Republic of Korea.

Supporting Information Available: Figure S1 of an ORTEP plot of $[Cu_3(\mathbf{L})(\mu_3\text{-OH})]Cl_{0.5}(ClO_4)_{4.5}\cdot 1.5H_2O$ and Figures S2−S7 for plots of magnetization data (11 pages). X-ray crystallographic files, in CIF format, for the complexes **1** and **2** are available through the Web only. See any current masthead page for ordering information and Web access instructions.

JA9721780

(11) K_a was obtained using $A_{obsd} = \epsilon_{OH}°[Cu_3]_t + (\epsilon_O° - \epsilon_{OH}°)[Cu_3]_t/(1 + [H^+]/K_a)$ where A_{obsd} is the observed absorbance and $[Cu_3]_t$ is the total concentration of Cu_3 species. $\epsilon_{OH}°$ and $\epsilon_O°$ are the extinction coefficients of μ_3-OH and μ_3-O tricopper complexes, respectively.

(12) Anal. Calcd for $Cu_3C_{24}H_{58}N_{12}O_{20.5}Cl_5$: C, 23.81; H, 4.83; N, 13.88. Found: C, 23.75; H, 4.49; N, 14.21. ν(O−H−Cl): 2536, 2114, 2089 cm^{-1}. UV/vis (MeCN): 738 nm (ϵ = 657 cm^{-1} M^{-1}) and 660 nm (sh). $\Lambda_M(H_2O)$; 658 Ω^{-1} cm^2 M^{-1} for 1.14×10^{-4} M.

(13) Crystal data for **2**: $Cu_3C_{24}H_{58}N_{12}Cl_5O_{20.5}$, fw = 1210.7, cubic, space group $P2_13$, a = 20.447(2) Å, V = 8548.5(14) Å^3, Z = 8, d_{calcd} = 1.881 g cm^{-3}, μ(Mo Kα) = 1.885 mm^{-1}, R = 0.0536 (4σ data), and $wR(F^2)$ = 0.1272. Relevant bond distances (Å) and angles (deg): Cu(1)−O(1), 1.951(4); Cu(1)−N(1), 2.207(9); Cu(1)−N(2), 2.013(9); Cu(1)−N(3), 2.141(10); Cu(1)−N(4), 2.086(10); Cu(2)−O(2), 1.966(4); Cu(2)−N(1), 2.202(8); Cu(2)−N(2), 2.001(9); Cu(2)−N(3), 2.114(9); Cu(2)−N(4), 2.104(9); Cu(1)−O(1)−Cu(1), 112.8(3); O(1)−Cu(1)−N(2), 178.6(4); N(4)−Cu(1)−N(3), 124.5(4); N(4)−Cu(1)−N(1), 131.9(4); N(3)−Cu(1)−N(1), 101.7(4); Cu(2)−O(2)−Cu(2), 112.1(3); O(2)−Cu(2)−N(2), 178.2(3); N(4)−Cu(2)−N(3), 122.3(4); N(4)−Cu(2)−N(1), 133.3(3); N(3)−Cu(2)−N(1), 102.6(3).

(14) The data were corrected for diamagnetic contribution and temperature independent paramagnetism (1.8×10^{-4} cgsu).

(15) The χ_M values are field-dependent at temperatures near the maximum χ_MT (Figures S2 and S3, Supporting Information) and the long-range interaction was observed even under 5 Oe. There is no ferromagnetic impurity, evidenced by the zero intercept in the plot of magnetization vs applied field (Figure S4 a−c, Supporting Information). The fitted magnetization isotherms at the temperature with $\chi_M T$(max) to Brillouin function[4] indicates a $S = {}^3/_2$ ground state (Figure S5, Supporting Information).

(16) The thermal depopulation of low-lying Zeeman levels may be an alternative or additional reason for the turnover in $\chi_M T$ at low temperature.

(17) (a) Fieselmann, B. F.; Hendrickson, D. N.; Stucky, G. D. *Inorg. Chem.* **1978**, *17*, 1841. (b) Lines, M. E.; Ginsberg, A. P.; Martin, R. L.; Sherwood, R. C. *J. Chem. Phys.* **1972**, *57*, 1.

(18) Costes, J.-P.; Dahan, F.; Laurent, J.-P. *Inorg. Chem.* **1986**, *25*, 413.

(19) (a) Angaroni, M.; Ardizzoia, G. A.; Beringhelli, T.; Monica, G. L.; Gatteschi, D.; Mascopcchi, N.; Moret, M. *J. Chem. Soc., Dalton Trans.* **1990**, 3305. (b) Bailey, N. A.; Fenton, D. E.; Moody, R.; Scrimshire, P. J.; Beloritzky, E.; Fries, P. H.; Latour, J.-M. *J. Chem. Soc. Dalton Trans.* **1988**, 2817. (c) Hulsbergen, F. B.; Hoedt, R. W. M.; Berschoor, G. C.; Reedijk, J.; Spek, A. L. *J. Chem. Soc., Dalton Trans.* **1983**, 539.

(20) (a) Beckett, R.; Colton, R.; Hoskins, B. F.; Martin, R. L.; Vince, D. G. *Aust. J. Chem.* **1969**, *22*, 2527. (b) Beckett, R.; Hoskins, B. F. *J. Chem. Soc., Dalton Trans.* **1972**, 291.

(21) The antiferromagnetic $Cu_3(\mu_3$-OH) species previously reported have magnetic orbitals involving $d_{x^2-y^2}$ and Cu−O−Cu bridging angles of 106−109° while the present complexes utilize d_{z^2} orbitals and have more flattened Cu−O−Cu angles (112−113°).

(22) Meenakumari, S.; Tiwary, S.; Chakravarty, A. *Inorg. Chem.* **1994**, *33*, 2085.